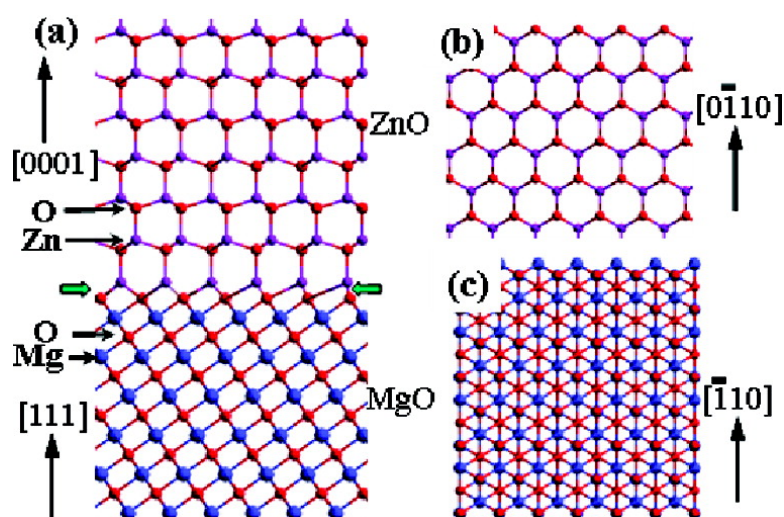


Growth of Crossed ZnO Nanorod Networks Induced by Polar Substrate Surface

J. H. He, C. H. Ho, C. W. Wang, Y. Ding, L. J. Chen, and Zhong L. Wang

Cryst. Growth Des., 2009, 9 (1), 17-19 • DOI: 10.1021/cg800530n • Publication Date (Web): 18 November 2008

Downloaded from <http://pubs.acs.org> on January 7, 2009



More About This Article

Additional resources and features associated with this article are available within the HTML version:

- Supporting Information
- Access to high resolution figures
- Links to articles and content related to this article
- Copyright permission to reproduce figures and/or text from this article

[View the Full Text HTML](#)



Growth of Crossed ZnO Nanorod Networks Induced by Polar Substrate Surface

J. H. He,^{*,†} C. H. Ho,[†] C. W. Wang,[‡] Y. Ding,[§] L. J. Chen,[‡] and Zhong L. Wang[§]

Institute of Photonics and Optoelectronics and Department of Electrical Engineering, National Taiwan University, Taipei, 106 Taiwan, Department of Materials Science and Engineering, National Tsing Hua University, Hsinchu, 300 Taiwan, and School of Materials Science and Engineering, Georgia Institute of Technology, Atlanta, Georgia 30332-0245

Received May 19, 2008; Revised Manuscript Received November 5, 2008

ABSTRACT: We show that by controlling the growth conditions, the crossed networks of ZnO nanorods were grown on an MgO (001) substrate. The [0001] ZnO nanorods grow along the $\langle 111 \rangle$ directions of MgO substrate and form aligned arrays. This growth is a result of polar surface induced growth from both the MgO {111} and ZnO \pm (0001). The crossed ZnO nanorod networks are a potential candidate for field emission, optoelectronics, ultrasensitive sensing, catalysts and filtering.

Wurtzite-structured ZnO is of great importance because of its versatile applications in optoelectronics, photovoltaics, and sensors.¹ Quasi-one-dimensional nanostructures of ZnO, such as nanowires, nanobelts, and nanotubes, have been a relevant research topic in nanotechnology for their unique properties and potential applications.^{2–7} As a wurtzite-structured oxide, zinc oxide is of three types and a total of 13 fastest growth directions: [0001], $\langle 01\bar{1}0 \rangle$, and $\langle 2\bar{1}\bar{1}0 \rangle$. Together with a pair of polar-surfaces such as {0001}, a unique group of novel nanostructures have been grown, such as asymmetric nanocantilever arrays,⁸ nanojunction-arrays,⁹ piezoelectric nanobelts,¹⁰ nanosprings,¹¹ and nanorings.¹²

Ordered nanorod networks are potential building blocks for memory and logic devices as well as interconnects, with the possibility of playing a key role in the future nanoscale electronics and optoelectronics.^{13–27} So far, a number of network structures have been grown for several different materials, including carbon nanotubes (CNTs), InP, GaP, Se, and Si.^{15,18–22} Because of the extremely small size of nanorods, organizing nanorods into ordered patterns by direct manipulation is slow and difficult. To solve this problem, researchers have demonstrated a few techniques based on an assembly method under the control of external forces. Chemical vapor deposition on patterned catalyst produced interconnected networks of CNTs.¹⁸ By employing microfluidics to align the nanorods within a lithographically defined channel, InP and GaP nanowires have been organized into cross arrays.¹⁹ Crossed networks of CNTs have been grown using electric-field-assisted deposition and orientation.²⁰ Template-directed CNT network formation using self-organized Si nanocrystals,²¹ three-dimensional Se nanowire networks,¹⁴ and Si nanowire networks controlled by the orientation of the substrate²² have been demonstrated. So far, several types of 3D ZnO nanostructures have been synthesized.^{26,27} For example, ZnO nanowires at the junctions of ZnO nanowalls have been synthesized. It demonstrated that 1D and 2D nanostructures with high crystallinity can be epitaxially and vertically grown into 3D architectures on both conducting and insulating single-crystalline substrates.²⁶ Moreover, ZnO nanowire arrays can be obtained with each nanowire forming an angle $\sim 30^\circ$ with the *m*-sapphire substrate normal by taking advantage of the good epitaxial interface between the (0001) plane of ZnO and the (1120) plane of the sapphire.²⁷ Because of the high surface/volume ratio, 3D oxide nanorod networks have been demonstrated as a high-surface-area material for building ultrasensitive and highly selective gas sensors.²³

In this communication, we report the growth of crossed nanorod networks of ZnO on MgO. The structure of the crossed ZnO networks is characterized, and its formation process is explained on the basis of polar surfaces for both the substrate and the ZnO. The photoluminescence (PL) spectrum of ZnO nanowire networks exhibits a strong emission peak at 386 nm. The 3D crossed ZnO network reported here could be important for applications in the transistor, optoelectronics, field emission, filtering, catalysis, and gas sensing.

Experimental Section. In the vapor–liquid–solid (VLS) growth, a 2 nm thick Au thin film was deposited onto the (001) MgO substrates at room temperature in an electron beam evaporation system at a pressure of $\sim 5 \times 10^{-6}$ Torr. Upon heating, the Au nanoparticles served as the catalyst for the VLS growth. The experimental apparatus includes a horizontal tube furnace, a rotary pump system, and a gas supply system. A mixture of commercial ZnO and graphite powders in a 4:1 Zn:C ratio was placed in an alumina boat, which was heated to a peak temperature of 1100 °C. The MgO substrate was placed at a temperature zone of ~ 800 °C for collecting ZnO nanostructures. After the tube had been evacuated to a pressure of 1×10^{-3} Torr, the samples were heated to 1100 °C at a rate of 5 °C/min and held at 1100 °C for 30–120 min with a mixture of 25 sccm Ar and 5 sccm O₂ flowing through the tube.

After the growth process, the resulting product was collected for phase identification using grazing incidence X-ray diffractometry (XRD) with a fixed incident angle of 0.5°. The substrate-bound nanorods were mechanically scrapped and sonicated in ethanol and deposited on carbon-coated copper grids for transmission electron microscope (TEM) characterization. Morphological studies of grown ZnO nanostructures have been performed with a JEOL 2010 TEM operating at 200 kV and a JEOL JSM-6500 field emission scanning electron microscopy (SEM). The PL properties of synthesized nanorods were studied at room temperature using a He–Cd laser with a wavelength of 325 nm as the excitation source.

Results and Discussion. For the samples cooled down to room temperature, the structure of the as-grown nanorods was determined by XRD. As shown in Figure 1, all of the diffraction peaks can be ascribed to the hexagonal-structured ZnO with the lattice constants of $a = 0.325$ nm and $c = 0.52$ nm, consistent with the standard data file (ICDD-PDF36–1451). No characteristic peaks from other phases were observed.

For the samples heated to 1100 °C and held at 1100 °C for 30 min, self-oriented ZnO nanowires were grown on the Au-deposited (001)MgO substrate, as shown in Figure 2. Figures 2a is a top view SEM image of the ZnO arrays on the MgO substrates. Figure 2b shows a cross-sectional SEM image of the sample with the viewing

* To whom correspondence should be addressed. E-mail: jhhe@cc.ee.ntu.edu.tw.

[†] National Taiwan University.

[‡] National Tsing Hua University.

[§] Georgia Institute of Technology.

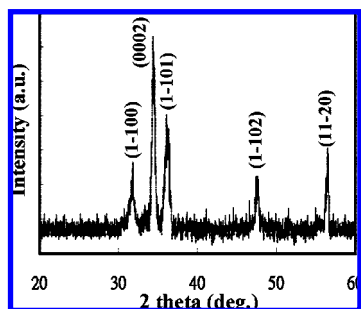


Figure 1. XRD pattern recorded from the as-synthesized products.

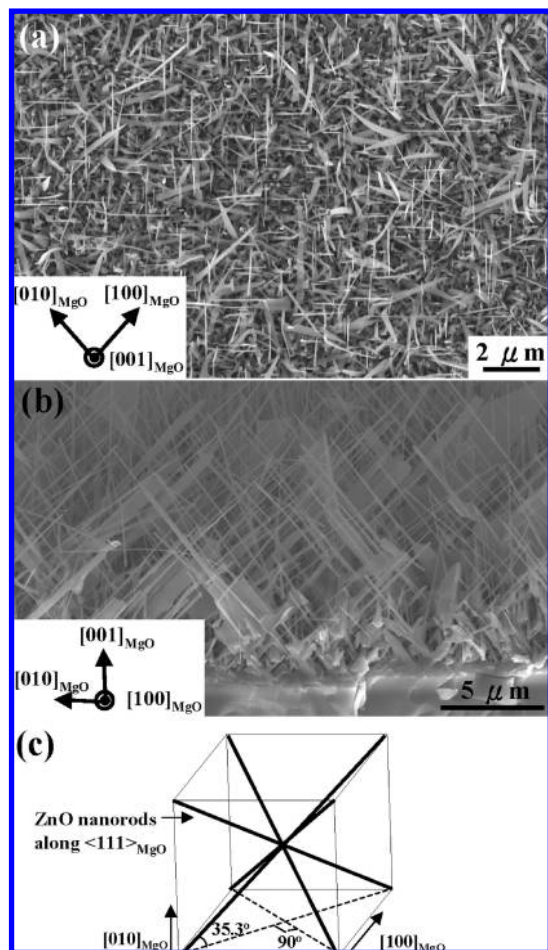


Figure 2. (a) Plan-view SEM image with the viewing direction $[001]_{\text{MgO}}$ and (b) cross-sectional SEM image with the viewing direction of $[100]_{\text{MgO}}$ of the ZnO arrays grown on an $(001)_{\text{MgO}}$ substrate and (c) schematic illustration of the four $\langle 111 \rangle_{\text{MgO}}$ growth directions of the ZnO nanowires on an $(001)_{\text{MgO}}$ substrate. Dashed lines represent the projections of the ZnO nanorods, which are perpendicular to each other.

direction of the $[100]_{\text{MgO}}$. The relative crystal orientations are shown in the insets of a and b in the Figure 2. It is clear that these ZnO nanorods formed crossed networks. In addition, beltlike ZnO nanostructures were also formed. From the information provided by images a and b in Figure 2, the ZnO nanorods grow along the $\langle 111 \rangle$ direction of the MgO substrate, as shown schematically in Figure 2c. In the present study, there are four directions of the growth for ZnO nanowire on the MgO substrates, which is a result of polar surface induced growth. In contrast, crossed ZnO nanowire networks on *m*-sapphire substrates were obtained by taking

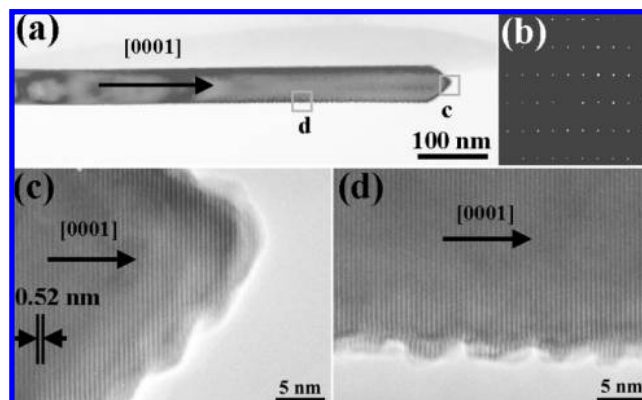


Figure 3. (a) TEM image of a single ZnO nanowire, (b) corresponding selected area diffraction pattern, and (c, d) HRTEM images from the outlined areas in (a).

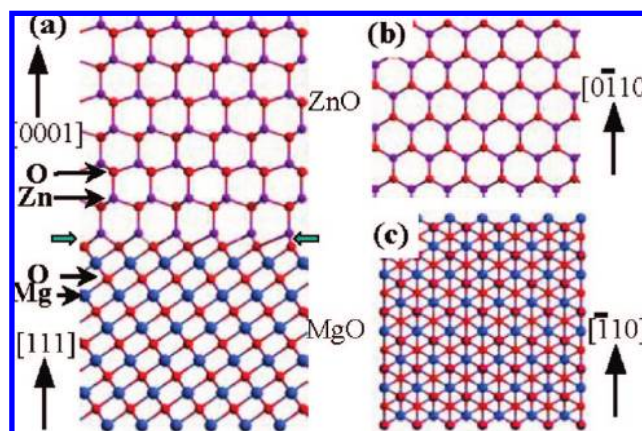


Figure 4. (a) $[10\bar{1}0]$ projection of the ZnO structure and $[01\bar{1}]$ projection of the MgO structure, showing $\pm(0001)$ polar surfaces of ZnO and $\pm(111)$ polar surfaces of MgO, respectively. (b) $[0001]$ projection of ZnO structure and (c) $[111]$ projection of MgO structure.

advantage of the good epitaxial interface between the (0001) plane of ZnO and the $(11\bar{2}0)$ plane of the sapphire.²⁷

TEM has been performed to further characterize the ZnO nanostructures. Figure 3a shows a typical TEM image of the single ZnO nanorod with a sharp tip. The diameter is about 50 nm. The corresponding selected area electron diffraction, as shown in Figure 3(b), confirms that the phase of nanorod is hexagonal wurtzite-structured ZnO. Images c and d in Figure 3 are high-resolution TEM (HRTEM) images from the outlined region indicated in Figure 3a. Images c and d in Figure 3 depicts that ZnO nanorods are single-crystalline and free of defects. The growth direction of ZnO nanorod was determined to be $[0001]_{\text{ZnO}}$.

To understand the growth orientation of the $[0001]$ ZnO nanorods on the $(001)_{\text{MgO}}$ substrate, we start from the structure of ZnO. ZnO has the hexagonal structure with $a = 0.325$ and $c = 0.52$ nm. ZnO can be simply viewed as composed of alternative layered Zn^{2+} and O^{2-} ions planes parallel to the basal plane. The (0001) and $(000\bar{1})$ surfaces of ZnO are terminated with Zn^{2+} and O^{2-} ions, respectively, which are known as the polar surfaces. MgO has the NaCl cubic structure with lattice parameter of $a = 0.421$ nm. The Mg^{2+} and O^{2-} ions are distributed alternatively in parallel to the $\{111\}$ plane, thus, the $\{111\}$ polar surface can be terminated either with Mg^{2+} or O^{2-} . The structure model of growth of $[0001]$ ZnO nanorods along the $\langle 111 \rangle_{\text{MgO}}$ direction is shown in Figure 4a. The structure models of the ZnO along $[0001]$ direction and MgO along $[111]$ direction are illustrated in images b and c in Figure 4. The (001) surface of MgO, however, is a nonpolar surface, thus a direct

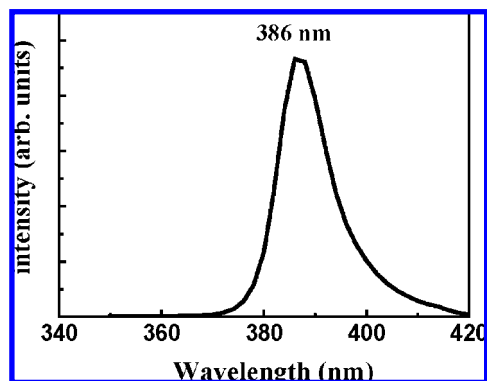


Figure 5. Photoluminescence spectrum of 2D rectangular ZnO nanowire network.

stacking of [0001] ZnO nanorod along [001]_{MgO} is restricted by the crystal symmetry, lattice mismatch as well as the surface charge. On the other hand, the (001)_{MgO} surface may be rough as a result of polishing, and it can exhibit tiny {111} type facets. Because of the polar charges on both MgO {111} and ZnO \pm (0001), a direct facing of ZnO (000 $\bar{1}$)–O²⁻ onto MgO (111)–Mg²⁺ would be a natural choice from the surface charge point of view. A previous work on the growth of ZnO thin films on sapphire substrate with MgO buffer layer also demonstrated the mechanism of polar-surface-induced growth.²⁸ Thus, the ZnO nanorod will grow along [0001] with the Zn-terminated surface in front. From our previous study,⁷ Zn terminated (0001) is self-catalytically active for nanorod growth, resulting in the growth of ZnO nanorods.

From the symmetry point of view, both (0001)_{ZnO} and (111)_{MgO} planes have 6-fold symmetry. The lattice mismatch between the two prominent planes {110}_{MgO} to {2 $\bar{1}$ 10}_{ZnO} is as high as 10.4%. This lattice mismatch is large enough to prevent the growth of large-size epitaxial films, but facilitate the formation of small size nuclei of ZnO leading eventually to the growth of nanorods.

Figure 5 shows a room-temperature PL spectrum of the crossed ZnO nanorod networks. There is a strong emission peak at 383 nm, corresponding to the near band edge emission of ZnO material. Encouraged by the recent demonstration of ultrasensitive and highly selective gas sensors using three-dimensional tungsten oxide nanowire networks,²³ a study on the gas sensing capability may yield very positive results. Furthermore, field emission, optoelectronic, and filtering performances of 3D crossed ZnO nanorod network should be explored since it appears as a promising material for such applications because of its unique nanostructure.

Conclusion. In summary, we show that by controlling the growth conditions, the crossed networks of ZnO nanorods were grown on an MgO (001) substrate. The [0001] ZnO nanorods grow along \langle 111 \rangle directions of MgO and form ordered arrays. This growth is a result of polar surface induced growth from both the MgO {111} and ZnO \pm (0001).

Acknowledgment. The research was supported by the National Science Council, Grants NSC 96-2112-M-002-038-MY3 and NSC 96-2622-M-002-002-CC3, and Aim for Top University Project from the Ministry of Education.

References

- (1) Heo, Y. W.; Norton, D. P.; Tien, L. C.; Kwon, Y.; Kang, B. S.; Ren, F.; Pearton, S. J.; LaRoche, J. R. *Mater. Sci. Eng., R* **2004**, *47*, 1.
- (2) He, H.; Lao, C. S.; Chen, L. J.; Davidovic, D.; Wang, Z. L. *J. Am. Chem. Soc.* **2005**, *127*, 16376.
- (3) Comini, E.; Faglia, G.; Sberveglieri, G.; Pan, Z. W.; Wang, Z. L. *Appl. Phys. Lett.* **2002**, *81*, 1869.
- (4) He, H.; Hsin, C. L.; Liu, J.; Chen, L. J.; Wang, Z. L. *Adv. Mater.* **2007**, *19*, 781.
- (5) He, J. H.; Lin, Y. H.; McConney, M. E.; Tsukruk, V. V.; Wang, Z. L.; Bao, G. *J. Appl. Phys.* **2007**, *102*, 084303.
- (6) Yu, C.; Hao, Q.; Saha, S.; Shi, L.; Kong, X. Y.; Wang, Z. L. *Appl. Phys. Lett.* **2005**, *86*, 063101.
- (7) He, J. H.; Ho, S. T.; Wu, T. B.; Chen, L. J.; Wang, Z. L. *Chem. Phys. Lett.* **2007**, *435*, 119.
- (8) Wang, Z. L.; Kong, X. Y.; Zuo, J. M. *Phys. Rev. Lett.* **2003**, *91*, 185502.
- (9) Lao, J. Y.; Wen, J. G.; Ren, Z. F. *Nano Lett.* **2002**, *2*, 1287.
- (10) Kong, X. Y.; Wang, Z. L. *Nano Lett.* **2003**, *3*, 1625.
- (11) Kong, X. Y.; Wang, Z. L. *Appl. Phys. Lett.* **2004**, *84*, 975.
- (12) Kong, X. Y.; Ding, Y.; Yang, R. S.; Wang, Z. L. *Science* **2004**, *303*, 1348.
- (13) He, J. H.; Hsu, J. H.; Wang, C. W.; Lin, H. N.; Chen, L. J.; Wang, Z. L. *J. Phys. Chem. B* **2006**, *110*, 50.
- (14) Cao, X. B.; Xie, Y.; Li, L. Y. *Adv. Mater.* **2003**, *15*, 1914.
- (15) Li, Q. C.; Kumar, V.; Li, Y.; Zhang, H. T.; Marks, T. J.; Chang, R. P. H. *Chem. Mater.* **2005**, *17*, 1001.
- (16) Ho, S. T.; Chen, K. C.; Chen, H. A.; Lin, H. Y.; Cheng, C. Y.; Lin, H. N. *Chem. Mater.* **2007**, *19*, 4083.
- (17) He, J. H.; Wu, T. H.; Hsin, C. L.; Li, K. M.; Chen, L. J.; Chueh, Y. L.; Chou, L. J.; Wang, Z. L. *Small* **2006**, *2*, 116.
- (18) Cassell, A. M.; McCool, G. C.; Ng, H. T.; Koehne, J. E.; Chen, B.; Li, J.; Han, J.; Meyyappan, M. *Appl. Phys. Lett.* **2003**, *82*, 817.
- (19) Huang, Y.; Duan, X. F.; Wei, Q. Q.; Lieber, C. M. *Science* **2001**, *291*, 630.
- (20) Yang, B.; Marcus, M. S.; Keppel, D. G.; Zhang, P. P.; Li, Z. W.; Larson, B. J.; Savage, D. E.; Simmons, J. M.; Castellini, O. M.; Eriksson, M. A.; Lagally, M. G. *Appl. Phys. Lett.* **2005**, *86*, 263107.
- (21) Diehl, M. R.; Yaliraki, S. N.; Beckman, R. A.; James, M. B.; Heath, R. *Angew. Chem., Int. Ed.* **2002**, *41*, 353.
- (22) Ge, S. P.; Jiang, K. L.; Lu, X. X.; Chen, Y. F.; Wang, R. M.; Fan, S. S. *Adv. Mater.* **2005**, *17*, 56.
- (23) Ponzoni, A.; Comini, E.; Sberveglieri, G.; Zhou, J.; Deng, S. Z.; Xu, N. S.; Ding, Y.; Wang, Z. L. *Appl. Phys. Lett.* **2006**, *88*, 20310.
- (24) Wu, Y.; Xi, Z. H.; Zhang, G. M.; Zhang, J. L.; Guo, D. Z. *Cryst. Growth Des.* **2008**, *8*, 2646.
- (25) Zhang, D. F.; Sun, L. D.; Zhang, J.; Yan, Z. G.; Yan, C. H. *Cryst. Growth Des.* **2008**, *8*, 3609.
- (26) Ng, H. T.; Li, J.; Smith, M. K.; Nguyen, P.; Cassell, A.; Han, J.; Meyyappan, M. *Science* **2003**, *300*, 1249.
- (27) Ng, H. T.; Chen, B.; Li, J.; Han, J. E.; Meyyappan, M.; Wu, J.; Li, S. X.; Haller, E. E. *Appl. Phys. Lett.* **2003**, *82*, 2023.
- (28) Kato, H.; Miyamoto, K.; Sano, M.; Yao, T. *Appl. Phys. Lett.* **2004**, *84*, 4562.

CG800530N